AFRL-RZ-WP-TP-2008-2194

PYLON FUEL INJECTOR DESIGN FOR A SCRAMJET COMBUSTOR (POSTPRINT)

Jason C. Doster, Paul I. King, Mark R. Gruber, and Raymond C. Maple

Propulsion Sciences Branch
Aerospace Propulsion Division

JULY 2007

AIR FORCE RESEARCH LABORATORY
PROPULSION DIRECTORATE
WRIGHT-PATTERSON AIR FORCE BASE, OH 45433-7251
AIR FORCE MATERIEL COMMAND
UNITED STATES AIR FORCE

REPORT DOCUMENTATION PAGE

Form Approved
OMB No. 0704-0188

1. REPORT DATE *(DD-MM-YY)*	2. REPORT TYPE	3. DATES COVERED *(From - To)*
July 2007	Conference Paper Postprint	01 August 2006 – 31 July 2007

4. TITLE AND SUBTITLE
PYLON FUEL INJECTOR DESIGN FOR A SCRAMJET COMBUSTOR (POSTPRINT)

5a. CONTRACT NUMBER
In-house

5b. GRANT NUMBER

5c. PROGRAM ELEMENT NUMBER
62203F

6. AUTHOR(S)
Jason C. Doster, Paul I. King, and Raymond C. Maple (Air Force Institute of Technology)
Mark R. Gruber (AFRL/RZAS)

5d. PROJECT NUMBER
3012

5e. TASK NUMBER
AI

5f. WORK UNIT NUMBER
3012AI00

7. PERFORMING ORGANIZATION NAME(S) AND ADDRESS(ES)
Air Force Institute of Technology
Wright-Patterson Air Force Base, OH 45433
Propulsion Sciences Branch (AFRL/RZAS)
Aerospace Propulsion Division
Air Force Research Laboratory, Propulsion Directorate
Wright-Patterson Air Force Base, OH 45433-7251
Air Force Materiel Command, United States Air Force

8. PERFORMING ORGANIZATION REPORT NUMBER
AFRL-RZ-WP-TP-2008-2194

9. SPONSORING/MONITORING AGENCY NAME(S) AND ADDRESS(ES)
Air Force Research Laboratory
Propulsion Directorate
Wright-Patterson Air Force Base, OH 45433-7251
Air Force Materiel Command
United States Air Force

10. SPONSORING/MONITORING AGENCY ACRONYM(S)
AFRL/RZAS

11. SPONSORING/MONITORING AGENCY REPORT NUMBER(S)
AFRL-RZ-WP-TP-2008-2194

12. DISTRIBUTION/AVAILABILITY STATEMENT
Approved for public release; distribution unlimited.

13. SUPPLEMENTARY NOTES
Conference paper presented at the 43rd AIAA/ASME/SAE/ASEE Joint Propulsion Conference and Exhibit, July 8 -11, 2007, in Cincinnati, OH.

PAO Case Number: WPAFB 08-5296; Clearance Date: 02 September 2008. This is a work of the U.S. Government and is not subject to copyright protection in the United States. Paper contains color.

14. ABSTRACT
This paper covers the initial development of an in-stream fuel injector concept for a circular hydrocarbon scramjet combustor. Three scramjet fuel injection pylon configurations are established–a basic pylon, a ramp pylon, and an alternating wedge pylon. The first pylon configuration is a baseline. The latter two configurations introduce streamwise vorticity into the flow to increase mixing action. Operating conditions and design considerations are discussed and the fuel injector configurations are presented. A testing methodology relating flight conditions to cold flow conditions is addressed. Initial Computational Fluid Dynamic simulations without fuel injection are presented for a wind tunnel cold flow test point. Two parameters used for comparison among the pylons are axial vorticity generation and total pressure loss. It is found the ramp and alternating wedge pylons increase streamwise vorticity in the flow over the basic pylon. The alternating wedge pylon increases streamwise vorticity the most. It is also found the ramp and alternating wedge pylons result in slightly increased total pressure losses due to the induced streamwise vorticity.

15. SUBJECT TERMS
Supersonic combustion, strut injection, flameholding

16. SECURITY CLASSIFICATION OF:			17. LIMITATION OF ABSTRACT:	18. NUMBER OF PAGES	19a. NAME OF RESPONSIBLE PERSON (Monitor)
a. REPORT	b. ABSTRACT	c. THIS PAGE			Mark R. Gruber
Unclassified	Unclassified	Unclassified	SAR	22	19b. TELEPHONE NUMBER *(Include Area Code)* N/A

Standard Form 298 (Rev. 8-98)
Prescribed by ANSI Std. Z39-18

43rd AIAA/ASME/SAE/ASEE Joint Propulsion Conference & Exhibit
8 - 11 July 2007, Cincinnati, OH

AIAA 2007-5404

Pylon Fuel Injector Design for a Scramjet Combustor

Jason C. Doster* and Paul I. King†
Air Force Institute of Technology, Wright-Patterson Air Force Base, OH 45433

Mark R. Gruber‡
Air Force Research Laboratory(AFRL/PRAS), Wright-Patterson Air Force Base, OH 45433

and

Raymond C. Maple§
Air Force Institute of Technology, Wright-Patterson Air Force Base, OH 45433

This paper covers the initial development of an in-stream fuel injector concept for a circular hydrocarbon scramjet combustor. Three scramjet fuel injection pylon configurations are established - a basic pylon, a ramp pylon, and an alternating wedge pylon. The first pylon configuration is a baseline. The latter two configurations introduce streamwise vorticity into the flow to increase mixing action. Operating conditions and design considerations are discussed and the fuel injector configurations are presented. A testing methodology relating flight conditions to cold flow conditions is addressed. Initial Computational Fluid Dynamic simulations without fuel injection are presented for a wind tunnel cold flow test point. Two parameters used for comparison among the pylons are axial vorticity generation and total pressure loss. It is found the ramp and alternating wedge pylons increase streamwise vorticity in the flow over the basic pylon. The alternating wedge pylon increases streamwise vorticity the most. It is also found the ramp and alternating wedge pylons result in slightly increased total pressure losses due to the induced streamwise vorticity.

I. Introduction

AFRL (Air Force Research Laboratory) is currently developing a scramjet combustor section with in-wall cavities to provide the needed residence time for hydrocarbon fuel/air mixing and ignition.[1–3] In addition to in-wall cavities AFRL is considering a circular combustor cross-section. This circular cross-section, having a low aspect ratio, presents challenges for effectively fueling the entire combustor area.

Fuel injection systems must mix fuel and air on both a large scale and small scale level. Mixing at the large scale is also called bulk mixing. Bulk mixing concerns the surface area interface between the fuel and oxidizer. Large turbulent eddies are primary flow structures responsible for bulk mixing. The larger the surface area interface achieved by large scale mixing, the faster fuel and oxidizer molecularly diffuses. Molecular diffusion results in small scale mixing. Small scale mixing is the goal, where fuel and oxidizer are brought to stoichiometric conditions at the molecular level so combustion can occur.

To be practical, the fuel injection system must accomplish molecular mixing with reasonable total pressure losses in an acceptable combustor length. Numerous fuel injection strategies have been studied.[4–6] The bulk of work in the early years of scramjet research was on parallel injection. Parallel injection produces a fuel/oxidizer shear layer with vortices oriented laterally to the combustor airflow.[7] Eventually, it was realized that shear layers of this sort resulted in long mixing times and combustor lengths. In addition,

*PhD Candidate, Dept of Aeronautics & Astronautics, Member AIAA
†Professor, Dept of Aeronautics & Astronautics, Senior Member AIAA
‡Senior Aerospace Engineer, AIAA Associate Fellow
§Assistant Professor, Dept of Aeronautics & Astronautics, Senior Member AIAA

as the difference in fuel and oxidizer flow speeds increased, compressibility effects degraded mixing further, leading to even longer mixing lengths. Pure parallel injection was an inefficient fuel/air mixing strategy.[8] Transverse injection to the combustor airflow was then studied to enhance mixing so reasonable combustor lengths could be achieved. Transverse injection creates a mixture of vortices with varied orientations to the combustor airflow. Mixing is enhanced with transverse injection, but total pressure losses are much higher than parallel injection.[8]

In order to attain the mixing efficiency of transverse injection and the milder total pressures losses of parallel injection, the next major thrust of research involved augmenting parallel injection with vortical structures oriented in the axial direction of the combustor airflow (streamwise vortices). Research on geometries that create streamwise vortices has shown promise and has led to the concept of the hypermixer, a device which induces mixing through the generation of streamwise vortices in a supersonic flow.[9] The two hypermixer geometries explored in this research are compression ramps and alternating wedges.

Injection downstream of compression ramps has been researched extensively.[10–14] The bulk mixing region just behind a ramp is dominated by large scale rotating vortices. The developed mixing region farther downstream is dominated by smaller scale turbulent vortices and diffusion. Two basic configurations, swept and unswept ramps, are prominent in the literature. Swept compression ramp designs create more vorticity, leading to enhanced mixing, but at a cost of higher total pressure loss.[4] Expansion ramps and a combination of compression/expansion ramps have also been researched.[5,15,16] The vortical motion behind all ramps is similar, but different ramp configurations lead to varying shapes and strengths of the axial vortices. In most studies swept ramp configurations, regardless of their compression/expansion geometries, result in stronger vortices and increased mixing capability.

More recently injection upstream of ramp configurations has been studied.[17–19] The advantage of injecting upstream of a ramp is the fuel and oxidizer meet prior to being entrained in the vortical structures generated by the ramp. This allows for more contact time and joint mixing action. Data obtained thus far shows promise for this injection strategy. One study compared upstream and base injection from a ramp and found upstream injection superior in mixing capability.[18] Upstream injection studies to date have used discrete circular fuel ports either ahead of or on top of a ramp configuration.

Alternating wedge geometries, setting up side-by-side compression and expansion areas, are another way of creating streamwise vortices.[20–22] Studies to date have incorporated alternating wedges that attach to a strut or a wall and inject fuel either from between the alternating wedges or from the alternating wedge vertexes.

There are other ways to increase fuel spreading/mixing. Fuel port geometry can have a significant affect. Circular fuel ports are most common. However, elliptical or rectangular fuel ports have exhibited superior mixing characteristics in experiments.[23–26] In general, fuel port geometries with elongated shapes exhibit better mixing characteristics over a circular geometry.[5] Elongated geometries increase the interface surface area of injected fluids whereas circular fuel port geometries minimize the surface area. Increased interface surface area allows for more rapid diffusion and mixing enhancement.

Research contained herein explores the advantages of thin film fuel injection upstream of a hypermixer to maximize the interface surface area of the fuel and combustor airflow. A very high aspect ratio rectangular slot fuel port greatly increases the perimeter to area ratio of the fuel stream. One hypermixer is a set of compression ramps. The other hypermixer is a set of alternating wedges.

In addition to properly mixing the fuel/air, the fuel injection system must also distribute fuel throughout the combustor cross-section. With the AFRL in-wall cavity concept some fuel injection is often necessary within the cavity to provide a sufficient heat source there; however, it is advantageous to have the bulk of the fuel/air mixture in the core combustor airflow to take advantage of all available oxygen. In addition, keeping the bulk of the heat release within the core airflow helps reduce combustor wall heating. Core airflow fuel injection has been studied at length and several fueling strategies have been used. Some of these include sidewall fuel injection, strut fuel injection, and pylon fuel injection. A strut is defined here as an in-stream geometric structure that spans the entire width or height of the combustor section and attaches to two walls. A pylon is an in-stream geometric structure that spans a portion of the combustor width or height and attaches to only one wall. Using in-stream struts and pylons as fueling devices is a very common practice in scramjet design. Much research is still being accomplished on strut designs.[16,18–22,27–33] Using pylons as fueling devices or components of fuel injection systems has also been studied by many researchers.[2,3,12,13,30,34–47] The way pylons are utilized varies. In many instances pylons are used as shields for fuel injector ports. In other instances pylons serve as housing structures for fuel injector ports.

The concept explored in this research of rectangular slot fuel injection upstream of a hypermixer is incorporated onto an in-stream pylon. The pylon facilitates fuel injection of gaseous hydrocarbon fuel into a supersonic airflow. The pylons studied in this research both house and shield fueling ports which inject fluid parallel to the combustor airflow.

II. Pylon Configurations

Three pylon configurations are studied: the basic pylon (Fig. 1), the ramp pylon (Fig. 2), and the alternating wedge pylon (Fig. 3). The construction of each pylon incorporates a two-piece front and back portion. The front portion contains a plenum common to all pylon configurations. The back portion contains a constant angled compression ramp in the case of the basic pylon, or a hypermixer geometry in the case of the other two pylons. The mating of the two halves creates the tall/thin rectangular injection slot (Fig. 1(b)) by the difference in the inner width of the front half and the outer width of the back half.

The common parameters for all pylons are:

- Height = 75 mm
- Length = 103 mm
- Frontal Blockage Area = 1215 mm^2
- Fuel Port (Slot) Area = 57 mm^2
- Front Wedge Angle = 14.7°
- Front Wedge Nose Radius = 1 mm

The basic pylon configuration embodies the fundamental fuel injection strategy of maximizing fuel interface area by using a rectangular slot injector spanning a large percentage of the pylon height. Figure 1 shows the basic pylon with a base attachment to insert the pylon into a combustor or wind tunnel wall. The back area of the basic pylon is a compression ramp at 10.6° (half angle) to the combustor airflow. For simplicity of design the fueling slots operate at sonic conditions. A plenum in the nose of the pylon provides fuel to the slots (Fig. 1(c)). This plenum is fed by an opening at the bottom of the pylon connected to the wall. The plenum also serves as a cooling sink for the front half of the pylon. Fuel injection is accomplished from a backward facing step that protects the injectant from the main flow for a short distance prior to meeting the combustor flow around the pylon.

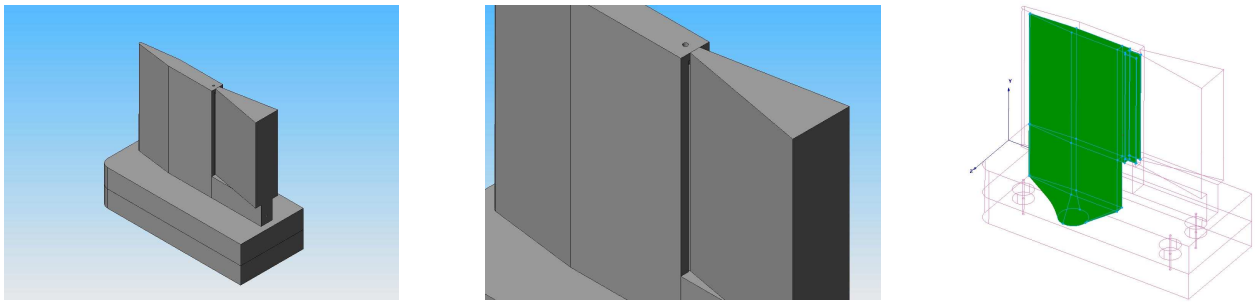

(a) External. (b) Rectangular fuel slot. (c) Internal.

Figure 1. Basic pylon configuration.

The ramp pylon configuration seen in Fig. 2 includes eight compression ramps on the back portion of the pylon. These compression ramps are 14.4° to the main airflow with 8.3° of sweep. The compression and sweep angles were chosen to produce the same frontal blockage area as the basic pylon configuration and have a sweep angle comparable to many past studies on swept ramps (about 10° of sweep). Past research has situated ramp injectors on combustor walls and struts. In one particular study fuel was injected downstream (from the base) of small unswept ramps placed on a pylon.[42] The design set forth in this paper injects fuel

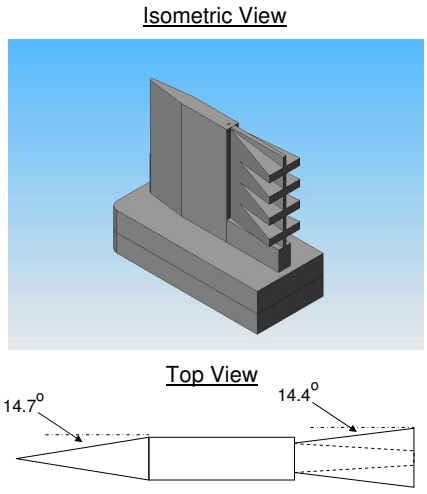

Figure 2. Ramp pylon configuration.

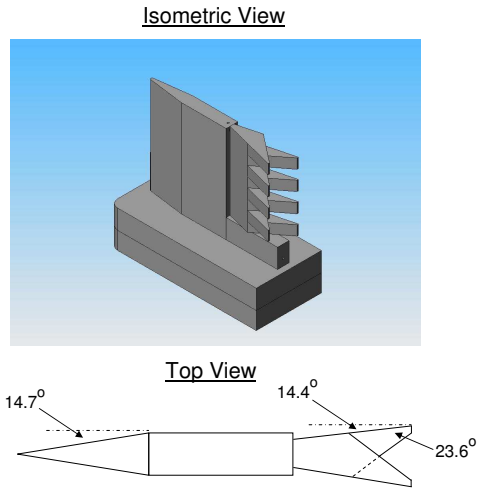

Figure 3. Alternating wedge pylon configuration.

upstream of numerous swept ramps on a pylon.

The alternating wedge configuration seen in Fig. 3 includes eight alternating wedges on the back portion of the pylon. This configuration is sized to produce the same frontal blockage area as the other two pylons. The wedge geometries have a 23.6° angle and attach to the back portion of the pylon, which itself has a 14.4° angle to the combustor airflow. This is the same compression angle used in the ramp pylon configuration. Past studies using alternating wedge geometries have injected fuel behind the wedges. The design set forth in this paper injects fuel just upstream of the wedges.

III. Pylon Design at Flight Conditions

In order to obtain a reasonable design for the pylons, the combustor environment and fuel injection requirements are addressed. A nominal 0.254 m circular cross-section is assumed and depicted in Fig. 4. The nominal fuel injection conditions are calculated given an eight pylon configuration. In addition, the wall thickness required to contain the plenum pressure and the area blockage due to the injectors are determined.

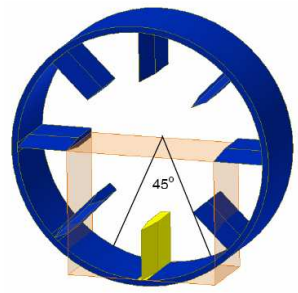

Figure 4. 0.254 m circular scramjet combustor.

Combustor Environment

A constant freestream dynamic pressure curve of 47,880 Pa (1000 lb/ft^2) is depicted in Fig. 5. This dynamic pressure trajectory is in the mid-range of that expected for a hypersonic vehicle.[8] Two specific points along this curve are chosen as flight condition cases. Inlet performance is obtained through a continuity and energy analysis assuming a kinetic energy efficiency of 0.97 and varying specific heat values with

temperature.[48] The area contraction ratio (freestream capture area divided by combustor area) chosen is approximately 10. The two flight cases are displayed in Fig. 6. Table 1 portrays the combustor inlet conditions for each flight condition case.

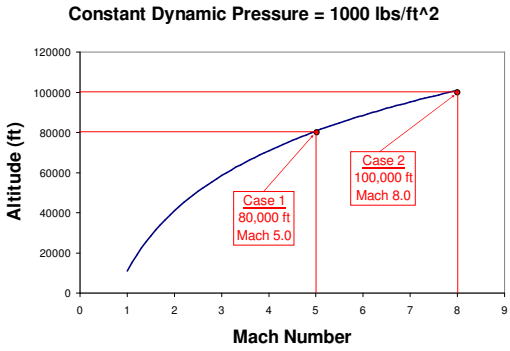

Figure 5. Dynamic pressure curve.

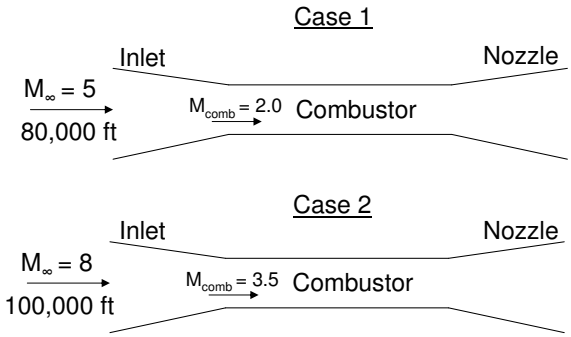

Figure 6. Two conditions chosen for analysis.

Table 1. Combustor inlet conditions.

Combustor Inlet Condition	Case 1	Case 2
Mach Number	2.0	3.5
Velocity	1054 m/s	2061 m/s
Mass Flow	30.8 kg/s	19.4 kg/s
Total Temperature	1224 K	2784 K
Static Temperature	712 K	901 K
Total Pressure	0.915 MPa	4.05 MPa
Static Pressure	118 KPa	48 KPa

Fuel Injector Requirements

The fuel injector requirements at the flight condition cases are sought. Three critical parameters include the amount of fuel mass flow required, the thickness of the pylon plenum walls required to contain the internal pressure, and the total blockage of the pylon structures in the combustor.

Fuel Injection

Three main assumptions are made. First, the pylons will supply the combustor with 75% of the necessary fuel to reach a global equivalence ratio of unity. This assumption is an upper limit to the amount of mass flow the pylons need to provide. AFRL combustor design includes the use of in-wall cavity flameholders downstream of the fueling pylons to provide the other 25% of the fuel. Second, eight fuel injection pylons will be utilized, each with a fueling port area of 57 mm^2. Third, the fuel, kerosene (approximated to be $C_{12}H_{26}$), is in a gaseous state and has the following bulk properties: a molecular weight of 170 g/mol, a specific heat ratio of 1.02, and stoichiometric ratio with air of 1:15 by mass.[48–51] The specific heat ratio is obtained assuming an ideal gas that has a molecular weight of 170 g/mol and a specific heat at constant pressure of 3000 J/(kg*K).

An unsteady isentropic code is used to accomplish pylon flow rate calculations. Kerosene begins to breakdown into smaller hydrocarbon chains (cracking) around 750 K,[51] but for calculations here the molecular weight, gas constant, and specific heat ratio of kerosene remain fixed. The code models the pylon as a constant area inflow, an ideal pressure vessel (the plenum), and a constant area outflow as seen in Fig. 7. It integrates the mass differential in the plenum from inflow and outflow and updates the plenum pressure until steady state is reached. The unsteady nature of the calculations reveals the time needed to pressurize the plenum area and obtain steady state mass flow from the pylon given instantaneous application of total

pressure and total temperature.

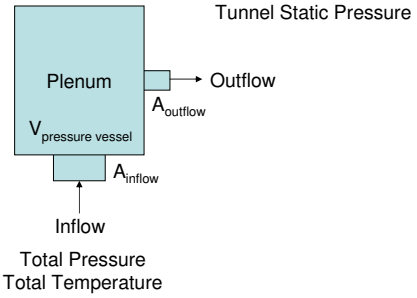

Figure 7. Pylon flow isentropic analysis.

Total fuel temperature is assumed to be 700 K for the case 1 flight condition and 900 K for the case 2 flight condition due to fuel cooling of the combustor walls.[48] For case 1, 30.8 kg/s of combustor airflow is expected. With a 1:15 stoichiometric ratio by mass, 75% fueling, and eight pylons, each pylon needs to deliver approximately 0.20 kg/s of fuel. For case 2, 19.4 kg/s of combustor airflow is expected. Each pylon needs to deliver approximately 0.13 kg/s of fuel. Table 2 portrays the fuel injector conditions given these parameters.

Table 2. Fuel injector conditions in combustor.

Fuel Injector Condition	Case 1	Case 2
Inflow Area	130 mm^2	130 mm^2
Inflow Total Pressure	1.05 MPa	0.80 MPa
Inflow Total Temperature	700 K	900 K
Plenum Gauge Pressure (Steady State)	889 KPa	719 KPa
Outflow Area	57 mm^2	57 mm^2
Outflow Mach Number	1.0	1.0
Outflow Velocity	186 m/s	211 m/s
Outflow Mass Flow	0.20 kg/s	0.13 kg/s

The total pressure required to achieve the fuel mass flow for case 1 is 1.05 MPa (152 psi / 10.4 atm), and for case 2 is 0.80 MPa (116 psi / 7.9 atm). This is the total pressure required from the scramjet's fuel circulation system. The steady state internal plenum gauge pressure of the pylon for case 1 is 889 KPa (129 psi/ 8.8 atm) and for case 2 is 719 KPa (104 psi/7.1 atm). These are the internal wall pressures the pylon must withstand to provide a sufficient mass flow to the combustor given the chosen configuration. For case 1 and case 2 the pylon plenum pressurization time is on the order of milliseconds.

The fuel mass flow from these calculations is compared to a vaporized kerosene mass flow study.[51] The difference in mass flow between the above calculations and data in the reference at the same total temperature, total pressure, and fuel exit area is within 1% for case 1 and 13% for case 2.

Structural Requirements

To accomplish a conservative analysis of the required plenum wall thickness a pylon plenum design gauge pressure of 500 psi is assumed. This is a safety factor of three over the maximum expected internal plenum pressure. A typical modulus of elasticity and yield stress for a high temperature resistant alloy in a thermal environment of 900 K is used. There is a reinforcing pin situated near the fuel port exit about half way up the plenum wall to ensure small deflections of the tall/thin rectangular slots. A two-dimensional grid of one side of the pylon is analyzed in NASTRAN with the specified gauge pressure. An adequate plenum wall thickness is found to be 2.5 mm (0.1 in) The maximum deflection (oil canning) along the slot injector wall is 8% of the slot width. The area increase of the slot due to deflection is roughly 4%.

Area Blockage

With the pylon wall thickness and inflow/outflow area requirements set, the pylon geometry can be established with some confidence that the dimensions are physically practical. All the pylon configurations are designed to have the same frontal area blockage. The frontal area of each pylon is 1215 mm^2. Eight pylons span the 0.254 m (50,670 mm^2) circular combustor cross section. This results in an overall combustor area blockage of 19.2%.

IV. Methodology

The pylon designs are first studied under cold flow conditions. Mach numbers and momentum ratios are the parameters matched between flight and cold flow conditions. Momentum flux ratio, $\bar{q}$, between the combustor airflow and the fuel flow is defined in Eq. 1. A substance close to the molecular weight and specific heat ratio of air is assumed as the notional fuel injectant simulant for cold flow studies.

$$\bar{q} \equiv \frac{\left(\gamma PM^2\right)_{\text{fuel injectant}}}{\left(\gamma PM^2\right)_{\text{combustor}}} = \frac{\left(\rho u^2\right)_{\text{fuel injectant}}}{\left(\rho u^2\right)_{\text{combustor}}} \tag{1}$$

Wind Tunnel Testing

Wind tunnel testing is planned; the condition matching between flight condition and cold flow is needed to run numerical simulations at the conditions expected in wind tunnel testing. Some initial numerical simulation results are discussed in following sections.

A variable throat supersonic wind tunnel located at the Air Force Institute of Technology (AFIT) is the chosen apparatus. The dimensions of the test section are 152.4 mm x 165.1 mm (25,161 mm^2). A single pylon is placed in the test section. The wind tunnel test section inlet Mach number matches the Mach number of the combustor inlet at flight condition. The expected wind tunnel test section inlet conditions are portrayed in Table 3.

Table 3. Wind Tunnel test section inlet conditions.

Combustor Inlet Condition	Case 1	Case 2
Mach Number	2.0	3.5
Velocity	518 m/s	654 m/s
Mass Flow	19.2 kg/s	4.8 kg/s
Total Temperature	300 K	300 K
Static Temperature	167 K	87 K
Total Pressure	552 KPa	552 KPa
Static Pressure	70.5 KPa	7.2 KPa

The momentum flux ratio between the pylon fuel stream and combustor airflow is also matched. For flight condition cases 1 and 2, the momentum flux ratios are approximately 1.0 and 0.6, respectively. The pylon operating conditions required to match these momentum flux ratios in wind tunnel cold flow are depicted in Table 4.

The pylon wind tunnel model does not have the same strength requirements of the actual flight hardware. The wind tunnel model pylon has the same dimensions as the flight designed pylon. The maximum plenum gauge pressure the wind tunnel model needs to withstand is approximately 440 KPa (64 psi).

V. Initial Numerical Simulations

FLUENT is the Computational Fluid Dynamics (CFD) code employed. Grid generation is accomplished using a combination of GRIDGEN and SOLIDMESH. A viscous grid is constructed around the pylons to the refinement required to utilize the boundary layer wall functions in FLUENT ($30 < y+ < 200$). The K-ω turbulence model with SST (shear stress transport) is used. The three pylon configurations employ different

Table 4. Fuel injector conditions in wind tunnel.

Fuel Injector Condition	Case 1	Case 2
Momentum Flux Ratio	1.0	0.6
Inflow Total Pressure	535 KPa	98 KPa
Inflow Total Temperature	300 K	300 K
Plenum Gauge Pressure (Steady State)	440 KPa	87 KPa
Outflow Velocity	317 m/s	317 m/s
Outflow Mass Flow	0.071 kg/s	0.013 kg/s

techniques of vortical generation with upstream parallel fuel injection. Their performance is compared. Only flow around the pylons without injection from the pylon is presented here. The primary performance parameters are the axial vortical intensity generated behind the pylon and the total pressure loss due to the pylon. The pylon external flow is solved with viscous and turbulent effects incorporated. The viscous solution sought is a second order steady state convergence of the Reynolds-averaged Navier Stokes equations. The case 1 flight condition simulation results are presented here.

Grid Construction

The exact dimensions of the AFIT wind tunnel are modeled with the pylon fixed to the bottom wall of the tunnel. The grid is hybrid in nature with a combination of structured/unstructured surface domains and tetrahedral/pentahedral cells. The size of each grid is 7.0 - 7.8 million cells. To mediate grid size the walls of the tunnel do not incorporate viscous spacing although they are designated as no-slip boundaries. A viscous grid is constructed around the pylon and the wake region is populated with a dense cell mesh. The cell volumes in the wake region are approximately 1 mm^3. The dense cell wake region extends 190 mm behind the pylon. Figure 8 depicts a typical grid.

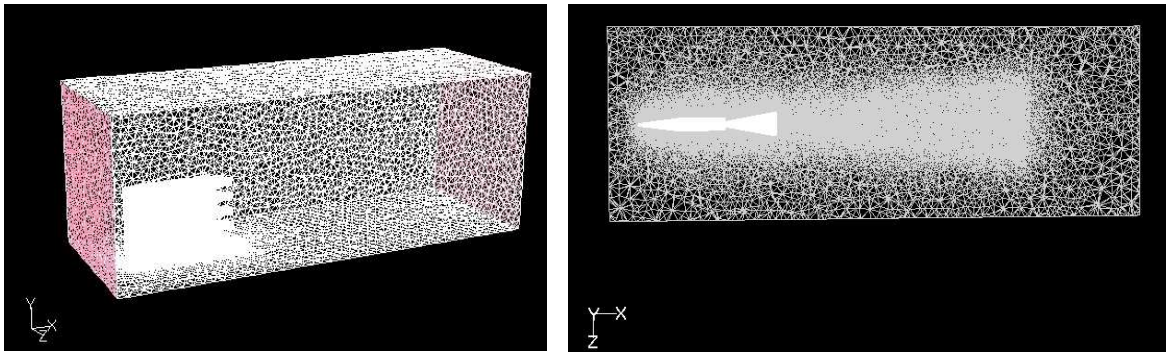

Figure 8. Typical CFD Grid.

The equivalent diameter, d_e, is the diameter of the rectangular slot fuel port area if it were to form a circle. The equivalent diameter for the fuel port area (57 mm^2) is 8.52 mm. The dense cell wake region therefore extends 22.3 equivalent diameters downstream of the pylon. Equivalent diameters is the nondimensional downstream distance used for all data presented here.

Convergence Criteria

The flow region behind the pylons is unsteady by nature, and the solver technique used here is a steady one. Four orders of magnitude reduction in velocity residuals and two orders of magnitude reduction in continuity residual was achieved. A more revealing convergence criteria is the pylon drag instead of the component residuals. Fifteen thousand iterations were adequate in all cases to obtain drag variation steadiness. Figure 9 depicts the drag convergence histories of each pylon configuration.

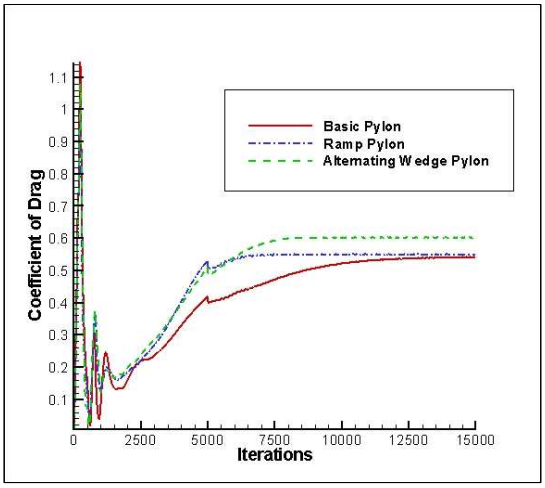

Figure 9. Drag convergence histories.

Basic Pylon

Selected CFD velocity solutions are shown in these subsections. CFD solution plots for each pylon configuration incorporate the same quantity ranges, Mach number or velocity, so visual comparisons can be made. Since the actual quantity ranges for each pylon are slightly different, the ramp and alternating wedge pylon solutions have places where no data are present (black) because the data are outside the range of the basic pylon which is used as the baseline. There are some common characteristics between all pylons. From the top views, two main compression shocks emanate, one from the front and one from the back where the compression ramps or turbulent generating devices are located. All pylons also have a low velocity base region in their wake. These base regions are of utmost interest for mixing potential. Each pylon has a different base region behavior. Even though injection is not accomplished in these solutions, the general behavior of the flow around and behind the pylons is assessed along with the drag and pressure losses due to the pylon structures.

Figure 10 depicts the basic pylon solution. The base region contracts down to a small concentrated low velocity region downstream of the pylon. The base region is very ordered and is not favorable for mixing. Subsonic flow extends downstream of the pylon approximately 11 d_e before transitioning to low supersonic flow. This long subsonic region allows for molecular communication, but there is very little if any bulk mixing from large vortical structures. Figure 11 emphasizes this point further by depicting streamlines flowing around the pylon from approximately 1 mm above the surface. These streamlines show little to no interaction behind the pylon. The streamlines simply follow the base region contraction with no significant perturbations.

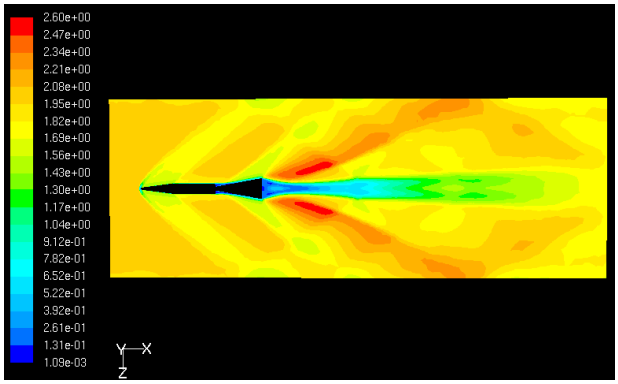

(a) Mach number: XZ plane (y = 45 mm).

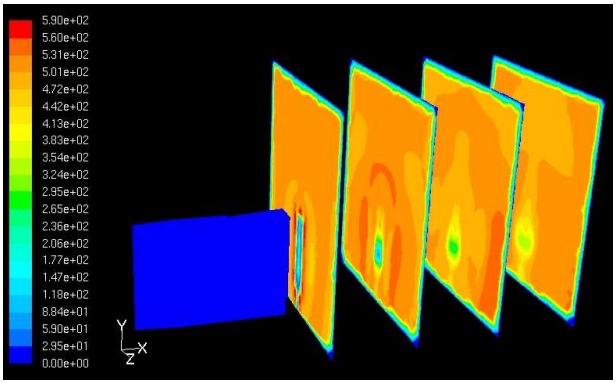

(b) Velocity magnitude (m/s): YZ planes ($1.2 < d_e < 22.3$).

Figure 10. Basic pylon flow.

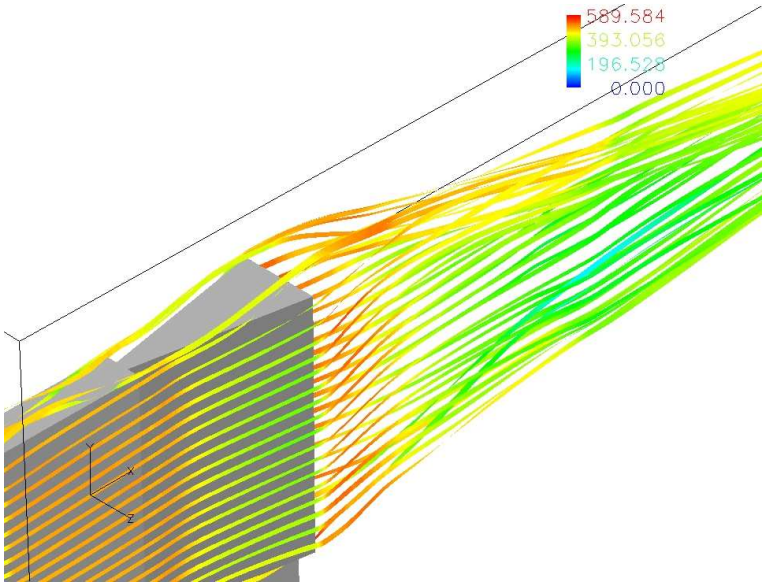

Figure 11. Basic pylon streamlines.

The non-dimensional measure of drag is the drag coefficient, which is defined in Eq. 2.

$$C_d = \frac{Drag}{\frac{1}{2}\rho u^2(Area)} = \frac{Drag}{\frac{\gamma}{2}PM^2(Area)} \tag{2}$$

The dynamic pressure multiplied by the pylon frontal area is 239.8 N for case 1 in wind tunnel cold flow. This is the same for all pylons since each has the same frontal area by design. The coefficient of drag for the basic pylon is 0.540. This translates to a drag of 130 N.

Ramp Pylon

The base area of the basic pylon is more uniform along the height of the pylon than the other configurations due to the uniform shape of the compression ramps. This is not so for the ramps and alternating wedges due to their non-uniform shapes. Recognizing this fact, but also wishing to be brief in the amount of visuals shown here, only one slice in the y-axis (height axis) will be displayed for the ramp and alternating wedge pylons at the same location as the basic pylon.

Figure 12 depicts the ramp pylon solution. Unlike the basic pylon, the base region of the ramp pylon does not have a contracting behavior in the downstream direction. The overall area of the lower velocity base region remains fairly constant, or even grows slightly, in the downstream direction. Vortices generated in the axial (x-axis) direction are apparent in Fig. 12b behind the pylon. This behavior is favorable for increased bulk mixing. It is also apparent in Fig. 12a the velocities in the base region are higher than the basic pylon base region velocities. Very little subsonic flow is observed here, favoring low supersonic speeds. This will inhibit molecular communication, possibly degrading small-scale molecular mixing.

Past studies have pointed to an increase in mixing potential with the generation of streamwise vortices. The ramp pylon configuration does generate axial vortices and appears to increase bulk mixing action in the near-field base region of the pylon. Streamlines depicted in Fig. 13 bolster this assertion. The streamlines flowing around the pylon approximately 1 mm above the surface have much more interaction with the base region. This is evident by the perturbations of the streamlines at the back of and behind the pylon.

The coefficient of drag for the ramp pylon is 0.549. This translates to a drag of 132 N compared to 130 N for the basic pylon.

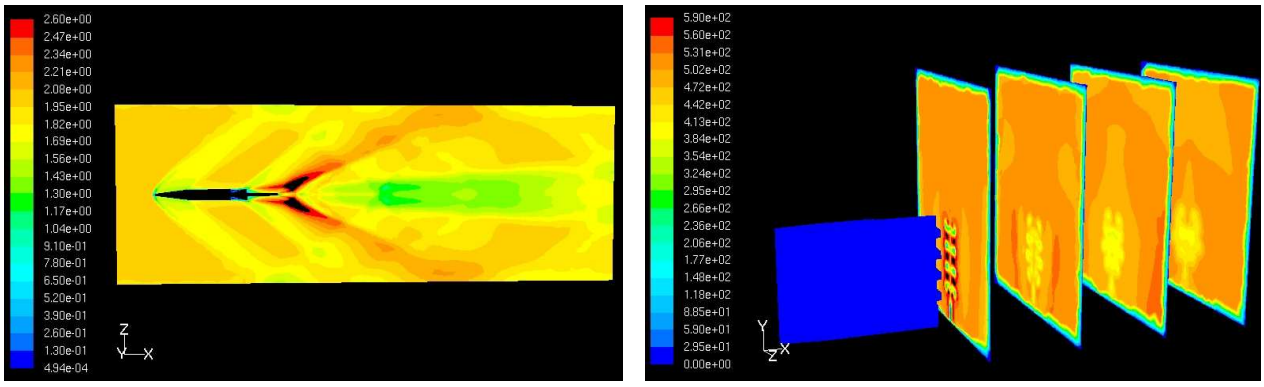

(a) Mach number: XZ plane (y = 45 mm). (b) Velocity magnitude (m/s): YZ planes ($1.2 < d_e < 22.3$).

Figure 12. Ramp pylon flow.

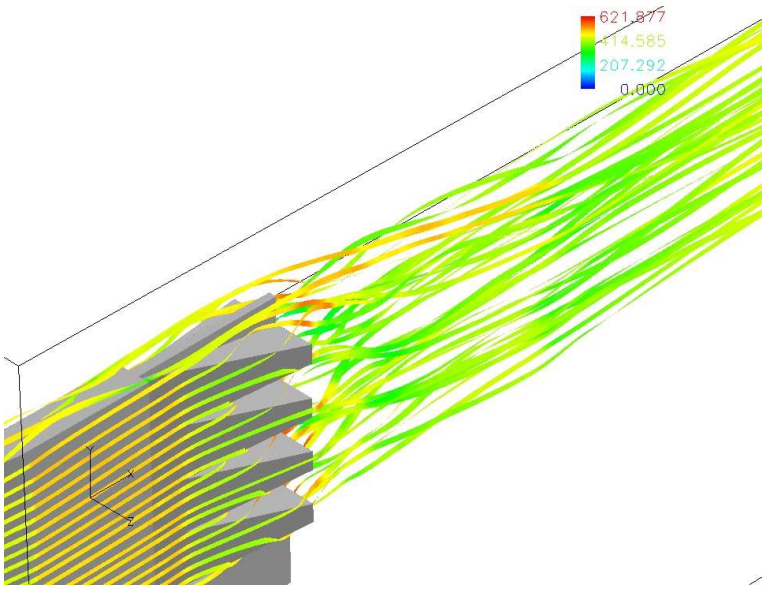

Figure 13. Ramp pylon streamlines.

Alternating Wedge Pylon

Figure 14 depicts the alternating wedge pylon solution. The behavior of this pylon is similar to the ramp pylon, but the vortical motion generated is more intense. The ramp pylon showed only small, if any, area increase of the low velocity base region in the downstream direction. The alternating wedge pylon has a definite base region area increase in the downstream direction. This pylon also generates stronger axial vortices than the ramp pylon. The mixing potential of this pylon appears to be the greatest of all the pylon configurations. Like the ramp pylon the velocity magnitudes behind this pylon are low supersonic with very little subsonic flow observed. The streamlines depicted in Fig. 15 also show much increased interaction between the flow around the pylon and the base region.

The alternating wedge pylon produces a noticeable increase in drag. The coefficient of drag for this pylon is 0.601. This translates to a drag of 144 N compared to 130 N for the basic pylon. The more intense vortical structures behind the pylon have increased the drag of the pylon.

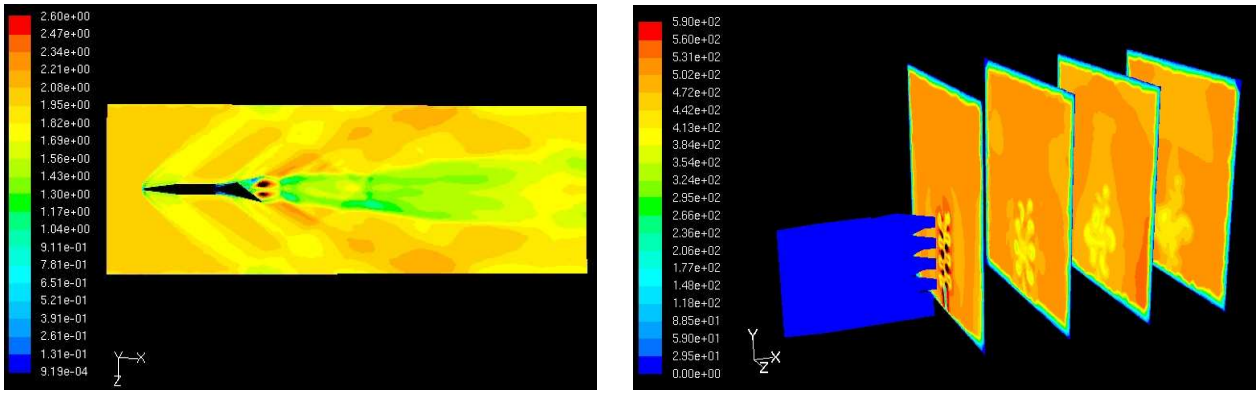

(a) Mach number: XZ plane (y = 45 mm). (b) Velocity magnitude (m/s): YZ planes ($1.2 < d_e < 22.3$).

Figure 14. Alternating wedge pylon flow.

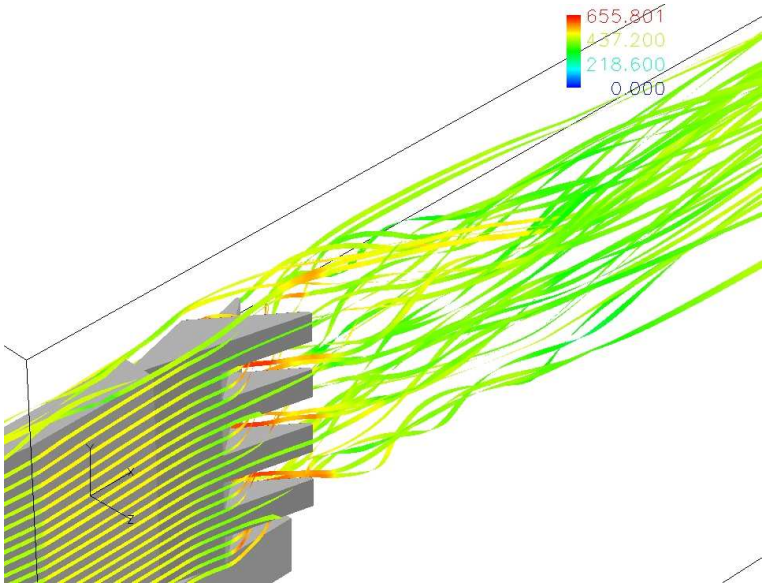

Figure 15. Alternating wedge pylon streamlines.

Additional Pylon Comparisons

Axial vorticity and total pressure loss are two parameters of comparison between the pylon configurations. Axial vorticity is a measure of the bulk mixing potential increase, and total pressure loss is the flow momentum loss due to the presence of the pylon. Each parameter is integrated over wind tunnel cross-sections at selected locations downstream of the pylon base. As a note, vorticity is directional and has positive and negative values. In order to integrate over a magnitude parameter which is always positive the absolute value of the x-vorticity is utilized and depicted in Eq. 3.

$$|\omega_x| \equiv \left| \left(\nabla \times \vec{V} \right)_x \right| \tag{3}$$

Since the walls of the tunnel are no-slip surfaces, there is some vorticity at the walls, and there is also total pressure loss due to the viscous walls. The walls of the tunnel are the same for every pylon configuration, so the relative differences between solutions are adequate to make comparisons. Integrated parameters at seven downstream locations ranging from 1.2 - 22.3 d_e are computed. A visual comparison of the x-vorticity at $d_e = 1.2$ is depicted in Fig. 16.

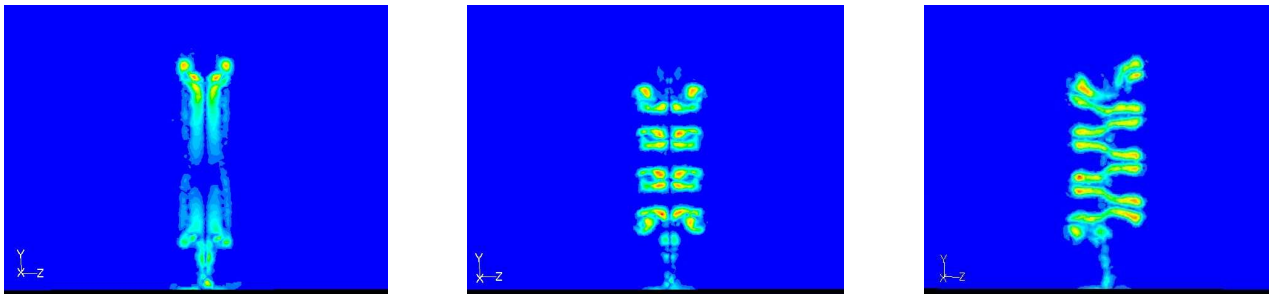

(a) Basic pylon. (b) Ramp pylon. (c) Alternating wedge pylon.

Figure 16. $|\omega_x|$ induced in wake region: d_e = 1.2.

It is visually evident that the ramp and alternating wedge pylon configurations induce more vortical motion in the axial direction than the basic pylon at the beginning of the base region. A more quantitative assessment is portrayed in Fig. 17. It is numerically evident that streamwise vorticity is increased overall with the ramp and alternating wedge geometries. The average axial vorticity increase of the ramp pylon over the basic pylon at all computed locations is 36%. The average axial vorticity increase of the alternating wedge pylon over the basic pylon at all computed locations is 88%. The basic pylon and ramp pylon have identical axial vorticity generation past 10 - 15 d_e downstream. The alternating wedge pylon exhibits more axial vorticity generation than the other two pylons at all calculated locations. The primary benefit of the hypermixing concepts appears to be in the near-field base region of the pylon.

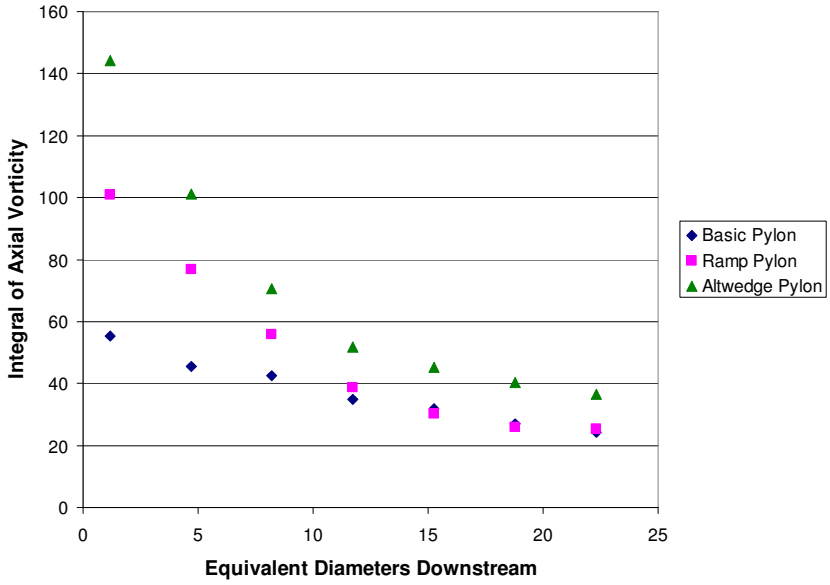

Figure 17. Integral of $|\omega_x|$ over cross-sections: (1.2 < d_e < 22.3).

$$\text{Total Presure Loss Ratio} = \frac{\text{Integrated Total Pressure at } d_e \text{ Behind Pylon}}{\text{Integrated Total Pressure Ahead of Pylon}} \tag{4}$$

The CFD (and wind tunnel) area blockage due to each pylon is 4.8% and the total pressure integrated over a cross-section just ahead of each the pylon is about 13,785 N. The total pressure loss ratio (Eq. 4) resultant from the three pylon configurations ranges around 0.93 - 0.95 (5% - 7% total pressure loss) depending on the location and pylon. Figure 18 compares the total pressure loss for each pylon. On average the basic pylon results in a 0.945 total pressure loss ratio, the ramp pylon results in a 0.943 total pressure loss ratio, and the alternating wedge pylon results in a 0.938 total pressure loss ratio. Both the ramp and alternating wedge pylons have less than a 1% decrease in total pressure loss ratio compared to the basic pylon. There

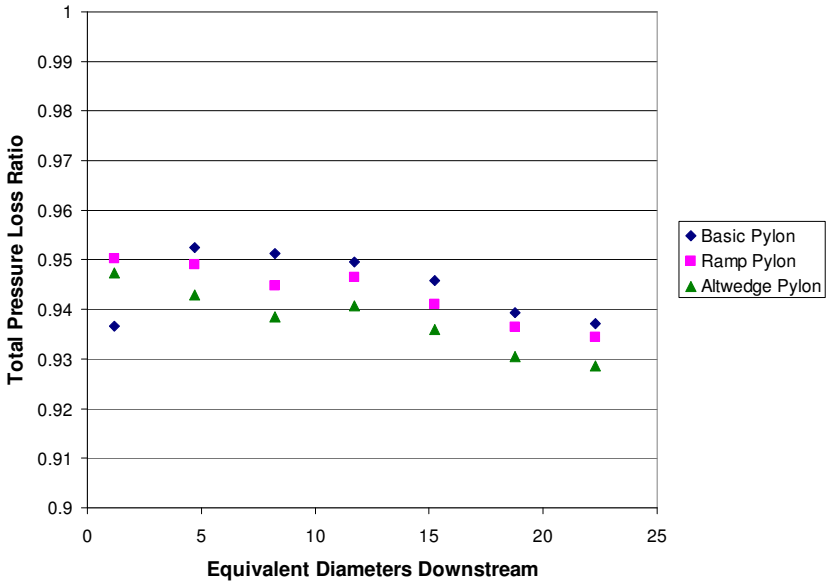

Figure 18. Total pressure losses: ($1.2 < d_e < 22.3$).

is a downward trend to the total pressure loss ratios with increasing downstream distance. This is due to a combination of factors including the shock train, viscous wind tunnel walls, and turbulent dissipation.

VI. Conclusions

Three pylon configurations are established as a class of in-stream scramjet fuel injectors. Cold flow CFD studies with no injection are accomplished on these pylon configurations. The ramp and alternating wedge pylons show decisive increases in axial vortical motion in the base region of the pylons with no additional frontal blockage area. The increase in vortical motion leads to some increase in drag and total pressure losses. In the case of the ramp pylon, for a 36% average increase in streamwise vorticity (as it is measured here by the integral over the wind tunnel cross-section of Eq. 3), the decrease in total pressure loss ratio is about 0.002. In the case of the alternating wedge pylon, for an 88% average increase in streamwise vorticity, the decrease in total pressure loss ratio is about 0.007. Axial vortical motion serves to increase the bulk mixing in the near-field base region of the pylon by adding interface surface area within the flow. The question remains if the increase in axial vortical motion directly translates also to increased mixing rates on the molecular level in the base region.

VII. Future Work

There is much work yet to be done. Simulant fuel injection must be added to the CFD cold flow solutions at the case 1 flight condition. In conjunction with numerical studies wind tunnel cold flow experiments at the case 1 flight condition will be accomplished. A case 2 flight condition cold flow analysis will follow. Once cold flow analysis is complete a multi-species CFD analysis with vaporized kerosene fuel at actual flight conditions may be accomplished.

The views expressed in this article are those of the author and do not reflect the official policy or position of the United States Air Force, Department of Defense, or the U.S. Government.

References

[1] *Powell, O., Edwards, J., Norris, R., Numbers, K., and Pearce, J., "Development of Hydrocarbon-Fueled Scramjet Engines: The Hypersonic Technology (HyTech) Program,"* Journal of Propulsion and Power*, Vol. 17, No. 6, Nov.-Dec. 2001,*

pp. 1170–1176.

[2] *Montes, D., King, P., Gruber, M., Carter, C., and Hsu, K., "Mixing Effects of Pylon-Aided Fuel Injection Located Upstream of a Flameholding Cavity in Supersonic Flow," AIAA Paper 2005-3913, Jul. 2005.*

[3] *Haubelt, L., King, P., Gruber, M., Carter, C., and Hsu, K., "Performance of Pylons Upstream of a Cavity-based Flameholder in Non-reacting Supersonic Flow," AIAA Paper 2006-4679, Jul. 2006.*

[4] *Bogdanoff, D., "Advanced Injection and Mixing Techniques for Scramjet Combustors,"* Journal of Propulsion and Power*, Vol. 10, No. 2, Mar.-Apr. 1994, pp. 183–190.*

[5] *Seiner, J., Dash, S., and Kenzakowski, D., "Historical Survey on Enhanced Mixing in Scramjet Engines,"* Journal of Propulsion and Power*, Vol. 17, No. 6, Nov.-Dec. 2001, pp. 1273–1286.*

[6] *Tam, C., Lin, K., and Raffoul, C., "Review of Jet-in-Crossflow Studies for Scramjet Application," Tech. rep., ARFL/PRAT, Wright Patterson Air Force Base, OH 45433, 2007.*

[7] *Murthy, S. and Curran, E.,* High-Speed Flight Propulsion Systems*, Vol. 137 of* Progress in Astronautics and Aeronautics*, American Institute for Aeronautics and Astronautics, 1991.*

[8] *Heiser, W. and Pratt, D.,* Hypersonic Airbreathing Propulsion*, Education Series, American Institute of Aeronautics and Astronautics, 1994.*

[9] *Curran, E. and Murthy, S.,* Scramjet Propulsion*, Vol. 189 of* Progress in Astronautics and Aeronautics*, American Institute of Aeronautics and Astronautics, 2000.*

[10] *Northam, G., Greenberg, I., and Byington, C., "Evaluation of Parallel Injector Configurations for Supersonic Combustion," AIAA Paper 89-2525, Jul. 1989.*

[11] *Riggins, D., Mekkes, G., McClinton, C., and Drummond, J., "A Numerical Study of Mixing Enhancement in a Supersonic Combustor," AIAA Paper 90-0203, Jan. 1990.*

[12] *Walther, R., Sabelnikov, V., Korontsvit, Y., Voloschenko, O., Ostras, V., and Sermanov, V., "Progress in the Joint German-Russian Scramjet Technology Programme," ISABE Paper 95-7121, Sep. 1995.*

[13] *Walther, R., Koschel, W., Sabelnikov, V., Korontsvit, Y., and Ivanov, V., "Investigations into the Aerothermodynamic Characteristics of Scramjet Components," ISABE Paper 97-7085, Sep. 1997.*

[14] *Aria, T., Sakaue, S., Morisaki, T., Kondo, A., Hiejima, T., and Nishioka, M., "Supersonic Streamwise Vortices Breakdown in a Scramjet Combustor," AIAA Paper 2006-8025, Nov. 2006.*

[15] *Waitz, I., Marble, F., and Zukoski, E., "Vorticity Generation by Contoured Wall Injectors," AIAA Paper 92-3550, Jul. 1992.*

[16] *Desikan, S. and Kurian, J., "Mixing Studies in Supersonic Flow Employing Strut Based Hypermixers," AIAA Paper 2005-3643, Jul. 2005.*

[17] *Kawano, S., Aso, S., and Orino, M., "A Study of a New Injector for Improvement of Supersonic Mixing," AIAA Paper 2000-0089, Jan. 2000.*

[18] *Shreenivasan, O., Kumar, R., Kumar, T., Sujith, R., and Chakravarthy, S., "Mixing in Confined Supersonic Flow Past Strut Based Cavity and Ramps," AIAA Paper 2004-4194, Jul. 2004.*

[19] *Manoharan, S., Chandra, B., Chakravarthy, S., Ramakrishnan, S., and Subramanyam, J., "Experimental Studies of Supersonic Cold Flow Mixing with Ramp Mixers,"* Journal of Aerospace Engineering*, Vol. 18, No. 4, Oct. 2005, pp. 197–205.*

[20] *Sunami, T., Wendt, M., and Nishioka, M., "Supersonic Mixing and Combustion Control Using Streamwise Vortices," AIAA Paper 1998-3271, Jul. 1998.*

[21] *Sunami, T. and Scheel, F., "Analysis of Mixing Enhancement Using Streamwise Vortices in a Supersonic Combustor by Application of Laser Diagnostics," AIAA Paper 2002-5203, Oct. 2002.*

[22] *Sunami, T., Magre, P., Bresson, A., Grisch, F., Orain, M., and Kodera, M., "Experimental Study of Strut Injectors in a Supersonic Combustor Using OH-PLIF," AIAA Paper 2005-3304, May 2005.*

[23] *Gutmark, E., Schadow, K., and Wilson, K., "Mixing Enhancement in Coaxial Supersonic Jets," AIAA Paper 89-1812, Jun. 1989.*

[24] *Zaman, K., "Spreading Characteristics and Thrust of Jets from Asymmetric Nozzles," AIAA Paper 96-0200, Jan. 1996.*

[25] *Haimovitch, Y., Gartenberg, E., Roberts, A., and Northam, G., "Effects of Internal Nozzle Geometry on Compression-Ramp Mixing in Supersonic Flow,"* AIAA Journal*, Vol. 35, No. 4, Apr. 1997, pp. 663–670.*

[26] *Gruber, M., Nejad, A., Chen, T., and Dutton, J., "Transverse Injection from Circular and Elliptical Nozzles into a Supersonic Crossflow,"* Journal of Propulsion and Power*, Vol. 16, No. 3, May-Jun. 2000, pp. 449–457.*

[27] *Scherrer, D., Dessornes, O., Montmayeur, N., and Ferrandon, O., "Injection Studies in the French Hypersonic Technologies Program," AIAA Paper 95-6096, Apr. 1995.*

[28] *Campbell, B., Siebenhaar, A., and Nguyen, T., "Strutjet Engine Performance,"* Journal of Propulsion and Power*, Vol. 17, No. 6, Nov.-Dec. 2001, pp. 1227–1232.*

[29] *Rocci-Denis, S., Maier, D., Erhard, W., and Kau, H., "Free Stream Investigations on Methane Combustion in a Supersonic Air Flow," AIAA Paper 2005-3314, May 2005.*

[30] *Gilinsky, M., Khaikine, V., Akyurtlu, A., Akyurtlu, J., Trexler, C., Baurle, R., Emami, S., and Blankson, I., "Numerical and Experimental Tests of a Supersonic Inlet Utilizing a Pylon Set for Mixing, Combustion and Thrust Enhancement," AIAA Paper 2005-3290, May 2005.*

[31] *Sunami, T., Itoh, K., Sato, K., and Komuro, T., "Mach 8 Ground Tests of the Hypermixer Scramjet for HyShot-IV Flight Experiment," AIAA Paper 2006-8062, Nov. 2006.*

[32] *Desikan, S. and Kurian, J., "Strut-Based Gaseous Injection into a Supersonic Stream,"* Journal of Propulsion and Power*, Vol. 22, No. 2, Mar.-Apr. 2006, pp. 474–477.*

[33] *Akyurtlu, A., Akyurtlu, J., Gonor, A., Khaikine, V., Cutler, A., and Blankson, I., "Numerical and Experimental Tests of a Supersonic Inlet with Pylon Set and Fuel Injection through Pylons," AIAA Paper 2006-1032, Jan. 2006.*

[34] *Avrashkov, V., Baranovsky, S., and Levin, V., "Gasdynamic Features of Supersonic Kerosene Combustion in a Model Combustion Chamber," AIAA Paper 90-5268, Oct. 1990.*

[35] *Naughton, J. and Settles, G., "Experiments on the Enhancement of Compressible Mixing via Streamwise Vorticity, Part I - Optical Measurements," AIAA Paper 92-3549, Jul. 1992.*

[36] *Rose, S. and Hartfield, R., "Experimental and Analytical Investigation of Injection Behind a Pylon in a Compressible Flow," AIAA Paper 96-0918, Jan. 1996.*

[37] *Sato, S., Izumikawa, M., Tomioka, S., and Mitani, T., "Scramjet Engine Test at the Mach 6 Flight Condition," AIAA Paper 97-3021, Jul. 1997.*

[38] *Semenov, V. and Romankov, O., "The Investigation of Operation Domain of Strut Fuel Feed System for Model Scramjet Combustor," AIAA Paper 98-1514, Apr. 1998.*

[39] *Gruenig, C. and Mayinger, F., "Supersonic Combustion of Kerosene/H2-Mixtures in a Model Scramjet Combustor," Tech. Rep. D-85747, Institute A for Thermodyamics, Technical University Munich, Garching, Germany, 1999.*

[40] *Gouskov, O., Kopchenov, V., Vinogradov, V., and Waltrup, P., "Numerical Researches of Gaseous Fuel Pre-Injection in Hypersonic 3-D Inlet," AIAA Paper 2000-3599, Jul. 2000.*

[41] *Livingston, T., Segal, C., Schindler, M., and Vinogradov, V., "Penetration and Spreading of Liquid Jets in an External-Internal Compression Inlet,"* AIAA Journal*, Vol. 38, No. 6, Jun. 2000, pp. 989–994.*

[42] *Gruenig, C., Avrashkov, V., and Mayinger, F., "Fuel Injection into a Supersonic Airflow by Means of Pylons,"* Journal of Propulsion and Power*, Vol. 16, No. 1, Jan.-Feb. 2000, pp. 29–34.*

[43] *Gruenig, C. and Mayinger, F., "Experimental Investigation of Supersonic Flame Stabilization based on Fuel Self-Ignition,"* Chemical Engineering Technology*, Vol. 23, No. 10, Oct. 2000, pp. 909–918.*

[44] *Owens, M., Mullagiri, S., Segal, C., and Vinogradov, V., "Effects of Fuel Preinjection on Mixing in Mach 1.6 Airflow,"* Journal of Propulsion and Power*, Vol. 17, No. 3, May.-Jun. 2001, pp. 605–610.*

[45] *Shikhman, Y., Vinogradov, V., Yanovski, L., Stepanov, V., Shlyakotin, V., and Pen'kov, S., "The Demonstrator of Technologies - Dual Mode Scramjet on Hydrocarbon Endothermic Fuel," AIAA Paper 2001-1787, Apr. 2001.*

[46] *Vinogradov, V., Shikhman, Y., Albegov, R., and Vedeshkin, G., "Experimental Research of Pre-Injected Methane Combustion in High Speed Supersonic Airflow," AIAA Paper 2003-6940, Dec. 2003.*

[47] *Vinogradov, V., Shikhman, Y., and Segal, C., "Review of Fuel Pre-Injection Studies in a High Speed Airflow," AIAA Paper 2006-1030, Jan. 2006.*

[48] *Curran, E., "Scramjet Engines: The First Forty Years,"* Journal of Propulsion and Power*, Vol. 17, No. 6, Nov.-Dec. 2001, pp. 1138–1148.*

[49] *"Aviation Fuel Properties," Tech. Rep. 530, Coordinating Research Council, 219 Perimeter Center Parkway, Atlanta, GA 30346, May 1988.*

[50] *Glassman, I.,* Combustion*, Academic Press, 1996.*

[51] *Fan, X., Yu, G., Li, J., Zhang, X., and Sung, C., "Investigation of Vaporized Kerosene Injection and Combustion in a Supersonic Model Combustor,"* Journal of Propulsion and Power*, Vol. 22, No. 1, Jan.-Feb. 2006, pp. 103–110.*